

1 **Characterisation of the Combustion Behaviours of Individual Pulverised** 2 **Coal Particles Entrained by Air Using Image Processing Techniques**

3 Xiangchen Qian^{1,*}, Fengjie Li¹, Yong Yan², Gang Lu², Hao Liu³

4 ¹ School of Control and Computer Engineering, North China Electric Power University, Beijing
5 102206, China

6 ² School of Engineering and Digital Arts, University of Kent, Canterbury, Kent CT2 7NT, UK

7 ³ Faculty of Engineering, University of Nottingham, University Park, Nottingham NG7 2RD, UK

8 * Corresponding author: xqian@ncepu.edu.cn

9 **Abstract**

11 The combustion characteristics of individual coal particles are the basis for a deep
12 understanding of the macroscopic pulverised coal combustion in power plant boilers. This work
13 proposes a quantitative method to characterise the combustion behaviours of individual
14 pulverised coal particles by measuring a set of physical parameters from digital images of the
15 particles. The combustion process of pulverised particles of bituminous coal in a visual drop tube
16 furnace was recorded by a high-speed camera with a frame rate of 6200 frames per second. An
17 improved-Canny algorithm was developed to extract the combustion zones of a coal particle in
18 both the volatile and char combustion phases. Using the improved-Canny and Otsu algorithms,
19 the unburned part of the particle was identified in the volatile combustion phase. Characteristic
20 parameters of coal particles, including the area, brightness, length, width and aspect ratio of
21 volatile flame, and falling velocity, were derived from the processed images. The results obtained
22 show that the volatile and char combustion took place successively and the volatile matter was
23 combusted almost as soon as it was released. The particle travelled upward for around 14 ms
24 during the early stage of combustion due to the influence of devolatilisation and volatile
25 combustion. The particle also exhibited a slight difference in the rotation frequency at different
26 combustion phases.

27
28 **Keywords:** Coal combustion, Coal particle, Drop tube furnace, Imaging, Image processing

29 **1. Introduction**

31 Coal-fired power generation accounts for 40% of the world's total electric power supply [1].
32 However, the use of coal has brought a series of environmental problems. A large amount of
33 hazardous emissions from coal-fired power plants has led to runaway greenhouse effects and
34 severe air pollution. Therefore, improving the power generation efficiency of coal-fired power
35 plants can not only save the depleting primary energy source of coal but also reduce the adverse

1 impacts of its use on the climate, environment and health. A quantitative and refined analysis of
2 the combustion characteristics of individual coal particles is extremely valuable to the
3 development of efficient and clean coal combustion technologies in coal-fired power plants.

4 Many factors influence the combustion of coal particles [2–4], such as particle size and
5 structure, chemical composition, furnace temperature, combustion environment composition
6 ($O_2/CO_2/N_2$), etc. Considering the complexity of an oxidation process, various simplified
7 combustion models have been established for simulation to obtain combustion data information
8 for the prediction of particles' combustion behaviours [4–6]. The single-film model [4], double-
9 film model [4], continuous-film model [4, 5] and shrinking core model [6] are commonly used in
10 previous studies. The latter two models have been proved to be more accurate and closer to the
11 real situation [4]. However, the accuracy of simulation results always needs to be verified and
12 supported by experimental studies. For example, the experiment results of the combustion
13 characteristic of single coal particles in a laminar flow field explored by Köser *et al.* [7] provided
14 certain data support for the simulation results of Farazi *et al.* [8]. Among various experimental
15 studies, thermogravimetric analysis (TGA) [9] and visualisation methods [10–21] are the most
16 commonly utilised to analyse the combustion behaviours of single solid fuel particles. However,
17 the TGA method can only obtain the mass loss variation parameters of the fuel. In contrast, the
18 visualisation method can directly observe the whole process of combustion and obtain more
19 comprehensive information.

20 In the last two decades, extensive experimental work has been carried out using different kinds
21 of solid fuels on visual drop tube furnaces (V-DTF) under various conditions. Shaddix *et al.* [11]
22 found that an increase in CO_2 concentration in the combustion atmosphere will delay the ignition
23 time of coal particles and prolong the burning time of volatiles using an intensified CCD camera.
24 Based on the images captured from a high-speed and high-resolution camera, Riaza *et al.* [14]
25 concluded that the ignition temperature of coal particles increases with carbon content and varies
26 with the ratio of N_2 , O_2 and CO_2 in the combustion atmosphere. More direct analyses on the
27 morphological changes of fuel particles during combustion was achieved through the combination
28 of a high-speed cinematography with three-colour pyrometers by obtaining the temperature-time-
29 size histories of different coal and biomass particles during combustion [3]. Lee *et al.* [15, 16]
30 conducted a series of quantitative studies based on the images of coal particles burned in a hot
31 rising gas stream. They conducted in-depth research on the motion of single coal particles using
32 interval images [15] and calculated relevant combustion parameters using image processing
33 algorithms [16]. The full use of the information contained in the images achieved a more detailed
34 analysis of solid fuel combustion. Bai *et al.* [17] extracted the surface roughness parameter and
35 the rotation frequency of the coal particle using the Otsu algorithm. Sarroza *et al.* [18] calculated
36 the distance between the position where the fuel started to ignite in the furnace and the top of the
37 furnace based on processed binary images. The support vector machine and deep learning

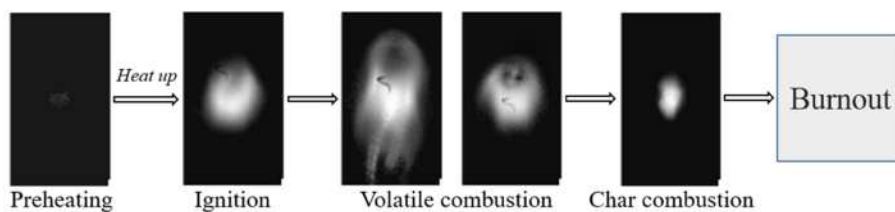
1 algorithms were adopted to establish an automatic system for the identification of the rank of coal
 2 based on the morphological features of the burning coal particle [19]. Wu *et al.* [20] and Yao *et*
 3 *al.* [21] obtained particle images from three directions and realised a multi-angle comprehensive
 4 analysis of burning coal particles utilising digital in-line holography. However, there is still much
 5 information contained in these digital images that have not been attended, such as displacement,
 6 structure, time, texture, etc., for the quantitative analyses of combustion behaviours of coal
 7 particles. Therefore, it is worthy of further research to reveal more characteristic information
 8 contained in the images of a burning fuel particle.

9 This paper proposes a quantitative method to characterise the combustion behaviours of
 10 individual coal particles in a V-DTF using image processing techniques. Consecutive images of
 11 the combustion process are recorded by a high-speed camera. An improved-Canny algorithm is
 12 developed to determine the whole combustion zone of a burning coal particle and to identify the
 13 unburned part of the particle during volatile combustion with the Otsu method. A set of
 14 characteristic parameters, i.e. area, length and width of the volatile flame, normalised average
 15 brightness, aspect ratio and falling velocity of the particle, is determined from the processed
 16 images to quantify the combustion behaviours of an individual coal particle.

17 2. Methodology

18 2.1. Combustion process of a coal particle

19 The combustion process of a coal particle can be categorised into four phases, i.e., drying
 20 (preheating), devolatilisation, volatile combustion and char combustion [2–4]. As shown in figure
 21 1, when a coal particle enters the combustion chamber of a boiler which is preheated to a
 22 temperature well above the coal particle ignition temperature, its body temperature rises rapidly
 23 by absorbing the heat from the surrounding gaseous environment. A V-DTF was used to simulate
 24 the combustion chamber in this study and its temperature was set at around 800°C as detailed in
 25 section 3. As the body temperature increases, the devolatilisation is followed, i.e., volatile matter
 26 is released from the coal particle. The volatile matter has a much lower ignition temperature
 27 (commonly 250°C to 450°C) in comparison to char (remaining coal particle after devolatilization)
 28 and thus ignites. As soon as the volatile matter burns out, the remaining char starts to burn as its
 29 temperature increases. Eventually, the particle burns out when all the volatile and carbon are
 30 oxidised.

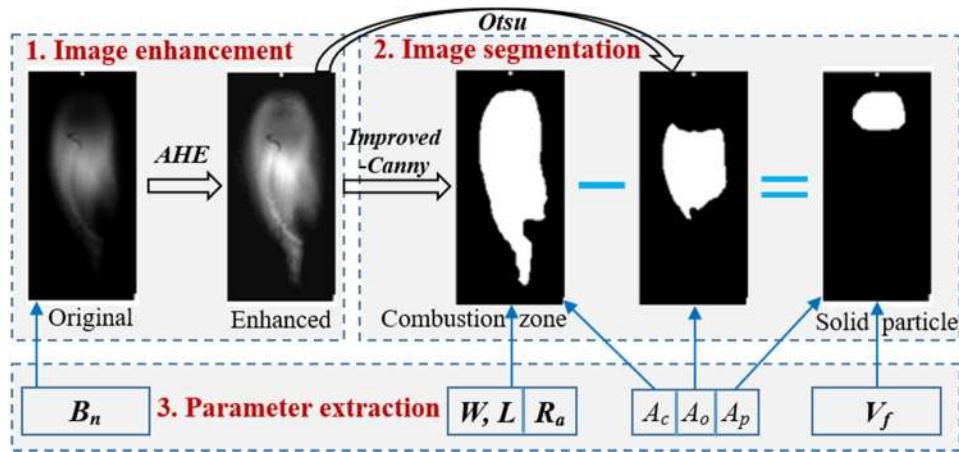


31 **Figure 1.** Flowchart of the combustion process of a coal particle.
 32

1 It should be noted, depending on many factors, for example, the conditions of the combustion
 2 chamber (temperature, composition of the combustion environment, etc.) and the coal properties
 3 (moisture content, particle size, rank, etc.), the four phases described above may overlap,
 4 especially the volatile combustion and char combustion phases.

5 2.2. Processing and analysis of burning particle images

6 With the aid of the high-speed and high-resolution image sensing technology, the above
 7 described combustion process of fuel particles can be visualised. Different image processing
 8 algorithms are applied to quantify the combustion characteristics of burning particles from the
 9 recorded images. Figure 2 shows the procedure of the image processing of a coal particle in this
 10 study, which mainly includes three steps, i.e., image enhancement, image segmentation and
 11 parameter extraction.



12
 13 **Figure 2.** Procedure of image processing of a burning coal particle.

14 2.2.1 Image enhancement

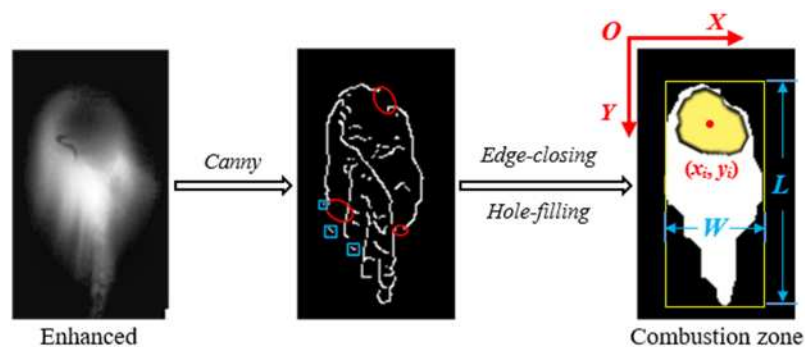
15 As the images of the burning particle captured by the camera commonly suffer from the
 16 problem of poor contrasting, image pre-processing techniques need to be applied to enhance the
 17 brightness and sharpness so that the combustion zones can be fully visualised. This is achieved
 18 by applying the adaptive histogram equalisation (AHE) algorithm [22] where the local histogram
 19 of the image is calculated to redistribute the brightness of the image to the full grey scale range
 20 (0-255 for an 8-bit image). Then different combustion zones, such as the whole combustion zone,
 21 combustion zone of volatile flame and combustion zone of char particle, are identified by the
 22 image segmentation. Finally, the characteristic parameters of a burning particle, such as area,
 23 brightness, length, width and aspect ratio of volatile flame, and falling velocity, are calculated for
 24 quantifying and characterising the combustion behaviours of the fuel particle during its
 25 combustion process.

26 2.2.2. Segmentation of combustion areas

27 A. Otsu and Canny algorithms

1 The Otsu and Canny algorithms are widely used for edge detection of images in many
 2 applications [10, 17, 18, 23–27]. The Otsu segmentation algorithm [23–25] is a commonly used
 3 adaptive threshold segmentation method to separate an image into two parts, the foreground
 4 (object, white, pixel value is 1) and the background (black, pixel value is 0). By traversing all the
 5 grey values of the pixels of the input greyscale image as a segmentation threshold, a series of
 6 inter-class variance between the foreground (white combustion zone) and background (black
 7 furnace wall) is obtained by each segmentation. Then the threshold corresponding to the
 8 maximum inter-class variance value is regarded as the optimal segmentation threshold. Finally,
 9 the optimal segmented binary image is obtained. The Otsu algorithm works well for solid
 10 particle images [30] as the grey value in the combustion zone (with a regular contour) is similar.
 11 However, as shown in figure 2, the processed results of the images with volatile combustion are
 12 poor as the Otsu algorithm is a single threshold method. Therefore, the Canny edge detection
 13 algorithm is employed to determine the contour of the combustion zone of the coal particle.

14 The Canny algorithm [26, 27] consists of three main steps. First, a Gaussian smoothing filtering
 15 is performed on the original image to reduce the detection error rate. Then, the gradient amplitude
 16 and gradient direction of the filtered image are calculated to evaluate the edge strength and
 17 direction at each pixel, and the gradient amplitude is non-maximum suppressed according to the
 18 gradient direction to identify finer edges. Finally, the pixels with a grey value lower than a low
 19 threshold are discarded, and the points with grey values greater than a high threshold as edge
 20 points. The pixels with a grey value between the low and high thresholds are determined to be the
 21 edge points using the eight-connected domain method. The Canny algorithm has a strong noise
 22 suppression capability and more accurate edge detection results as the identified edges are much
 23 thinner than other algorithms. However, the detected contour edges of a coal particle in the
 24 volatile combustion phase are mostly incomplete due to the influence of edge tips and the complex
 25 texture inside the combustion zone. As it can be seen from figure 3, there are many scattered
 26 points around the edges in addition to the breakpoints on the particle contour. To solve these
 27 problems, an improved object extraction algorithm by combining the Canny edge detection with
 28 edge-closing and hole filling functions (improved-Canny) is proposed in this study to obtain an
 29 enclosed contour of a burning particle from enhanced images.



30
 31

Figure 3. Procedure of the improved-Canny algorithm.

1 *B. Improved-Canny algorithm*

2 Firstly, an edge closing operation is carried out on the remaining edges to connect the narrow
3 discontinuities and long breaks in the contour line. First, the expansion processing is used to
4 “roughen” the combustion zone of the coal particle in the image and connect the breakpoints.
5 Then the corrosion treatment, which is the opposite operation of expansion, is performed to
6 shrink, refine and enclose the contour edges. As shown in figure 3, the small areas outside the
7 edges are removed from the image. At this stage, there are still many “holes” in the counter edges,
8 such as a small group of adjacent white-coloured foreground pixels and the small black-coloured
9 background areas surrounded by some white-coloured pixels. A hole-filling process [24, 25] is
10 performed by identifying the holes mentioned above and then set the colour of all the pixels of
11 the identified holes in the entire combustion zone. Then a binary image of the whole combustion
12 zone is obtained. A coal particle with high volatile content releases volatile matter intensely and
13 then burns in the initial volatile combustion phase. As the char particle has not reached its ignition
14 point at this stage, its brightness is relatively low in the images. As shown in figure 3, the top part
15 of the combustion zone, which is the unburned part of the coal particle, is dimmer in the original
16 and enhanced images. As it can be seen from figure 2, the Otsu algorithm is unable to distinguish
17 the high temperature zones from the whole combustion zone of the particle (determined by the
18 Canny algorithm). Therefore, the two algorithms are combined to extract the unburned zone of
19 the coal particle during devolatilisation. The particle image processed by the improved-Canny
20 algorithm is firstly “subtracted” by the Otsu-processed images, and then the unburned zone of the
21 particle is obtained by morphological image processing. In the char combustion phase, the
22 improved-Canny detection algorithm is applied to obtain the unburned part of the coal particle as
23 there is no/little interference of volatiles.

24 **2.3. Characteristic parameters of a particle**

25 Several geometric and luminous parameters can be defined and calculated to quantify the
26 dynamic characteristics of coal particles during the combustion process.

27 *Area (A)*: The area represents the projected region of particle acquired from the image. It is
28 calculated by counting the number of all the pixels of the projected region in the image, i.e.,

$$29 \quad A = p^2 \sum_{(x,y) \in R} 1, R \in I \quad (1)$$

30 where R is the projected region of particle acquired from the image I . Coefficient p is a factor of
31 the length to the corresponding pixel size and is determined according to the the configuration of
32 the image sensor used in the image acquisition (section 3.1).

33 *Normalised average brightness (B_n)*: The grey value of the image of the burning fuel particle
34 has a direct relationship to the radiative intensity of the combustion zone of the particle (subject
35 to the Planck’s Radiation Law). Only the region with the radiative intensity that is strong enough
36 to be visualised is regarded as the combustion zone. In order to quantify the brightness of the

1 combustion zone, B_n is defined as the average grey value of all the pixels in the whole combustion
 2 zone in the original image, and is normalised by the upper limit of grey value, i.e.

$$3 \quad B_n = \frac{1}{255} \sum_{(x,y) \in A} G(x,y) / A \times 100\% \quad (2)$$

4 where $G(x, y)$ is the grey value of the pixel at (x, y) ranging from 0 to 255.

5 *Equivalent Length and Width (L and W)*: The length and width can be very useful to
 6 characterise the shape of the volatile flame. However, the flame is irregular in shape. Equivalent
 7 length L and width W are defined as the height and width of the smallest rectangle which encloses
 8 the entire combustion zone I_c , as shown in figure 3, i.e.,

$$9 \quad L = pm_r \quad (3)$$

$$10 \quad W = pn_r \quad (4)$$

11 where m_r and n_r are the height and width of the smallest rectangle that envelops the combustion
 12 zone (figure 3), respectively.

13 *Aspect ratio (R_a)*: R_a is the ratio of the length and width of the volatile flame, reflecting the
 14 overall morphological changes of the flame. It is calculated as follows:

$$15 \quad R_a = L/W. \quad (5)$$

16 *Falling velocity (V_f)*: The falling velocity depicts the dynamic characteristics of the burning
 17 fuel particle which is essential in the study of the combustion behaviours of the particle suspended
 18 in the combustion atmosphere (preheated air in this study). It is calculated by tracking the centre
 19 of the char particle (figure 3) in an image sequence (not the small images shown in figures 1 to
 20 3). As the position of the high-speed camera is fixed, the displacement of the centre of the char
 21 particle (d_i) in the i^{th} image at every time point is calculated. Then the particle velocity can be
 22 obtained by taking the derivative of the fitting curve of d_i , as shown in the following formulas:

$$23 \quad d_i = \sqrt{(x_i - x_{i-1})^2 + (y_i - y_{i-1})^2} \quad (6)$$

$$24 \quad V_f = p \frac{d_i}{\tau} \quad (7)$$

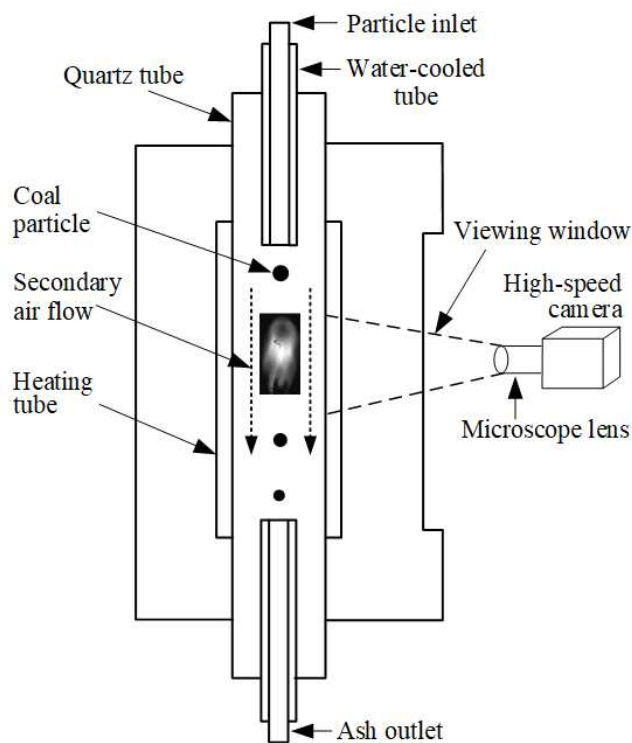
25 where (x_i, y_i) is the coordinate of the centroid of the solid particle in the i^{th} image and τ is the
 26 interval between two consecutive images.

27 **3. Results and discussion**

28 **3.1. Acquisition of coal particle images**

29 To examine the proposed methodology as described in section 2, a pre-recorded video clip of
 30 burning coal particles in a V-DTF using a high-speed camera system was used [17, 18], as shown
 31 in figure 4. The coal tested was the bituminous coal [17] commonly used in power generation and
 32 was obtained from a coal-fired power plant in pulverised form with an average size of about 75
 33 μm and the top size of 212 μm . Coal particles within the size range of 150 μm to 212 μm were
 34 used in the V-DTF tests to ensure problem-free particle feeding. The V-DTF used in this study is

1 an electrically heated vertical test furnace and a vertically oriented quartz tube (with an inner
 2 diameter of 50 mm and 1400 mm long) serves as the combustion chamber. In each test, a small
 3 amount (a few milligrams) of coal particles was manually dropped into the top inlet of the quartz
 4 tube that was pre-heated to 800°C through the water-cooled feeding tube without the use of a
 5 carrier gas but with the supply of the secondary combustion air flow at 5 L min⁻¹. The temperature
 6 of the quartz tube was chosen because it is below the maximum safe operating temperature of the
 7 quartz tube (1000°C) and within the range of the operating temperatures of a typical pulverised
 8 coal-fired furnace (about 500°C at the initial stage of coal injection and about 1200°C after coal
 9 combustion flames have been fully established). The particles were heated, ignited and combusted
 10 in the quartz tube with the residual ash being vacuumed away from the bottom end of the quartz
 11 tube. There is a viewing window at the front side of the furnace which allows the camera to view
 12 the combustion process of the coal particles inside the quartz tube. The high-speed camera
 13 (Phantom v12.1) coupled with a long-distance microscope (Questar QM-1) recorded the coal
 14 particles during their residence time in the furnace at a frame rate of 6200 frames per second (fps)
 15 with an image resolution of 720W×1280H pixels (in the field of view is about 8 mm × 8 mm).
 16 The imaging system was pre-calibrated before the tests so that the camera field of view could
 17 cover the main combustion process of the coal particle.



18
 19

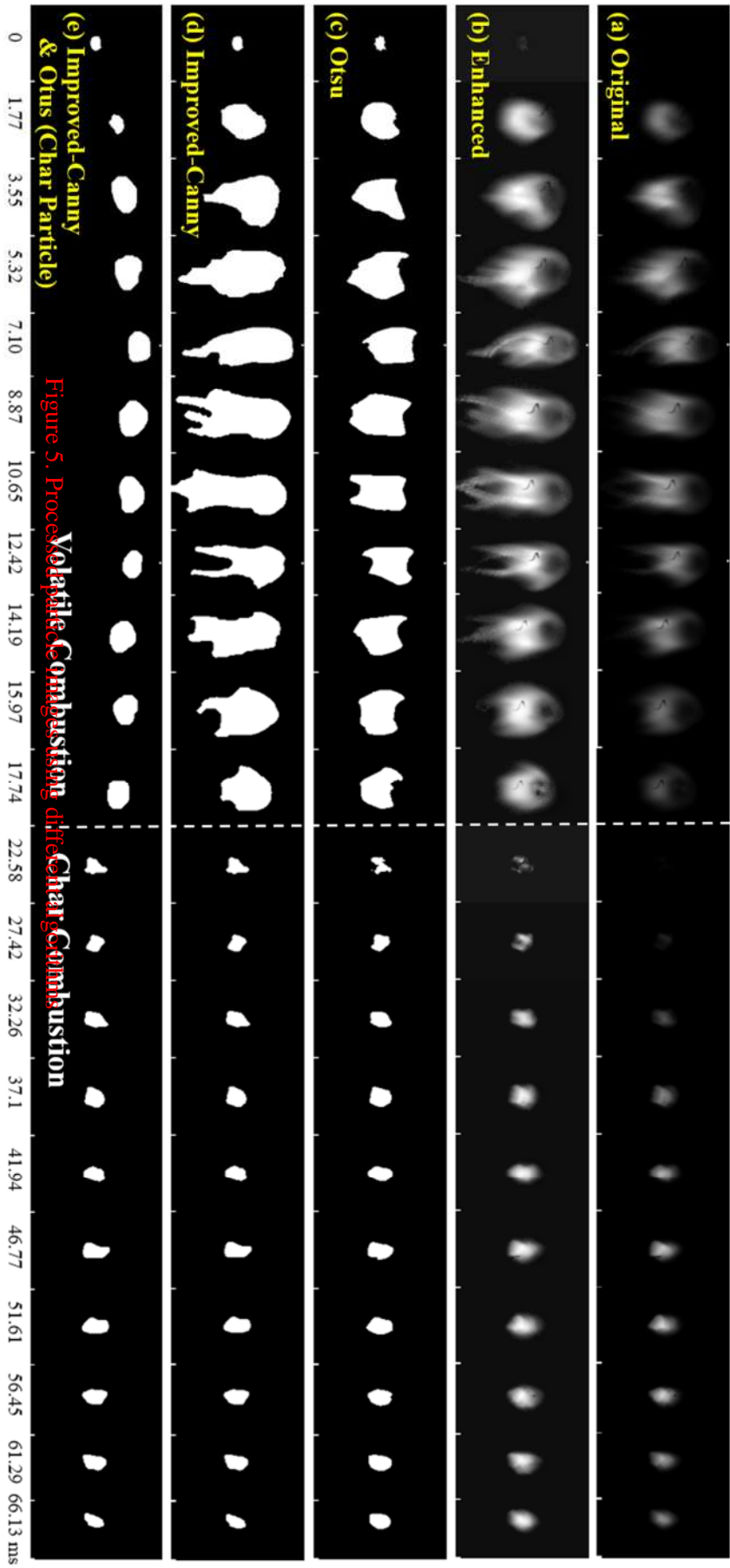
Figure 4. Schematic of the V-DTF experimental setup.

20 3.2. Segmentation of combustion zones in an image

21 The images shown in the top row of figure 5 are the example images of a coal particle extracted
 22 from the video. As it can be seen from figure 5, the images provide visualised information

1 associated with the combustion behaviours of the particle in their residence time. The particles
2 which appeared in the video were already in the combustion chamber (i.e. quartz tube) for some
3 time, and therefore, each image frame does not represent the absolute residence time of the
4 particle in the quartz tube. However, the relative residence time between different frames can be
5 obtained by referring to the residence time of two successive frames (0.16 ms). The combustion
6 of volatiles and char of the particles was clearly observed from the images. As described
7 previously, the segmentation of the combustion zones in the particle images is one of the crucial
8 steps in particle characterisation. This is particularly challenging due to the dynamic nature of the
9 burning coal particle in different combustion phases (section 2.1). As shown in figure 5, for
10 example, at the relative residence of 19.19 ms, the brightness of the burning particle was very low
11 and hardly observed. This process lasted for about 6.45 ms before the particle was visualised
12 again. This is believed to be due to the fact that there is a transient period between the volatile
13 release and volatile combustion phases of the coal particle. It should be noted that the total
14 combustion time of the coal particle is slightly longer than that being recorded by the video. The
15 current visualisation technique used in this study does not allow the tracking of the complete
16 combustion process of micro-scale fuel particles without the loss of resolving power (the smallest
17 area that can be identified).

18 The algorithms described in section 2.2.2 were examined for the segmentation of combustion
19 zones of particles in the images. As shown in figures 5(b), the burning particle can be better
20 identified in the enhanced images using the AHE algorithm. Compared with figures 5(a) and (c),
21 it can be found that the Otsu algorithm can only extract the brighter zones accurately, which is
22 consistent with the result that human eyes can observe from the original images. As shown in
23 figure 5(d), the proposed improved-Canny algorithm was used to determine the whole combustion
24 zone, including the dimmer top and tail of the volatile flame. Furthermore, the improved-Canny
25 algorithm can extract the edge of the burning char more accurately, and the influence of the image
26 brightness on the extraction of particle edge can be reduced in contrast with the former method.
27 The images of the coal particle shown in figure 5(e) were determined from figures 5(c) and (d)
28 (as introduced in section 2.2). As it can be seen from figure 5(e), the shape and size of the burning
29 particle change constantly. It is inevitable that the area of the unburned coal particle obtained by
30 the proposed method may be slightly affected by the volatile matter, especially in the volatile
31 combustion phase. However, it has proven that the improved-Canny algorithm outperformed
32 other edge detection algorithms in determining the geometric characteristics of the burning coal
33 particle from its images.



3.3. Combustion behaviours of a coal particle

3.3.1. Brightness

It can be observed from figure 6 that the brightness of the burning coal particle increased first and then decreased to almost zero after reaching a specific value. Then the particle became bright again after a short period of time. The two peaks of the normalised average brightness again indicate that the combustion of this particular bituminous coal is clearly divided into two successive phases. The sharp increase of brightness in the first 3 ms means the volatile gases released from the interior of the coal particle were burnt quickly as the ignition point of these volatile gases was low and easily reached. The brightness of the burning volatiles reached a peak at 3.4 ms and the whole volatile combustion lasted for about 22 ms. The brightness of the char changed dramatically in both ignition (22–44 ms) and burnout (56 ms to end). Such a phenomenon is owing to the composition of the char is mainly carbon. Therefore, the char started to burn from the “tips” on the surface and then spread to the whole char particle gradually [17]. In the periods of 4–11 ms and 44–57 ms, the average brightness fluctuates within a small range, illustrating that the combustion is in a relatively stable state. Moreover, the brightness of the volatile combustion is slightly lower than that of the char combustion, indicating the latter occurs at a higher temperature and produces more heat.

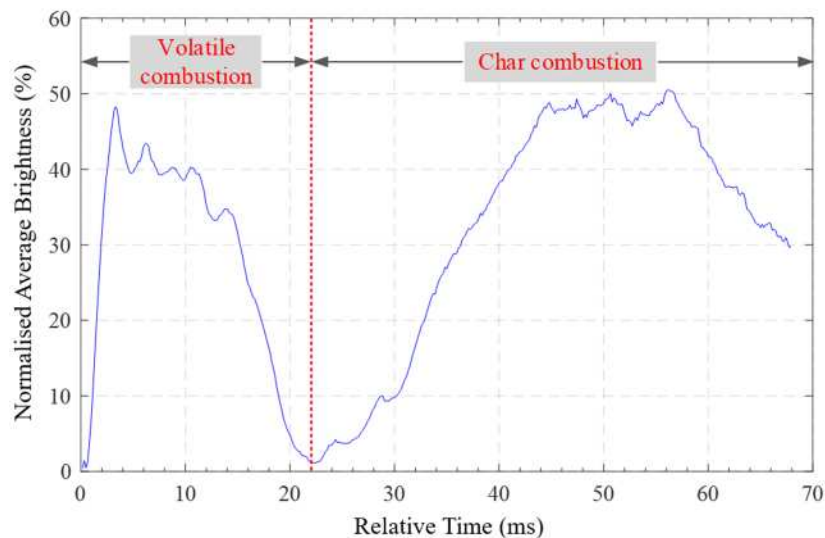
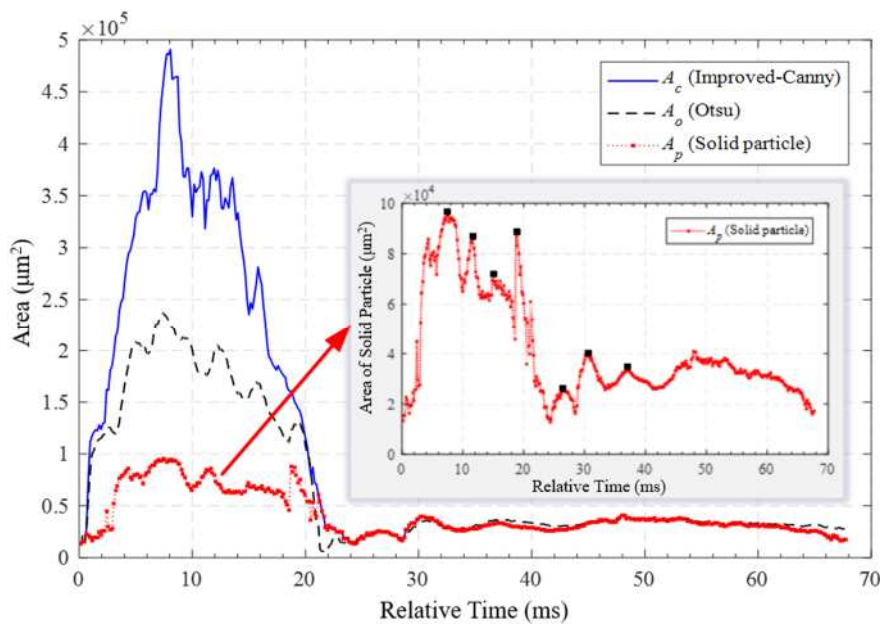


Figure 6. Normalised average brightness of the burning coal particle.

3.3.2. Geometrical characteristics

The variation of the combustion areas of the burning coal particle is shown in figure 7. The subscripts of A , i.e., c , o and p , are used to identify the different combustion areas, i.e., A_c - whole combustion zone (figure 5(d)), A_o - brighter zone of the volatile flame (figure 5(c)), and A_p - char combustion zone (figure 5(e)). The coefficient p of the images (equation (1)) is estimated to be $8.8 \mu\text{m pixel}^{-1}$ according to the configuration of the test rig and the microscope lens when the equivalent diameter (the diameter of a perfect circle of the same area) of the coal particle is 150

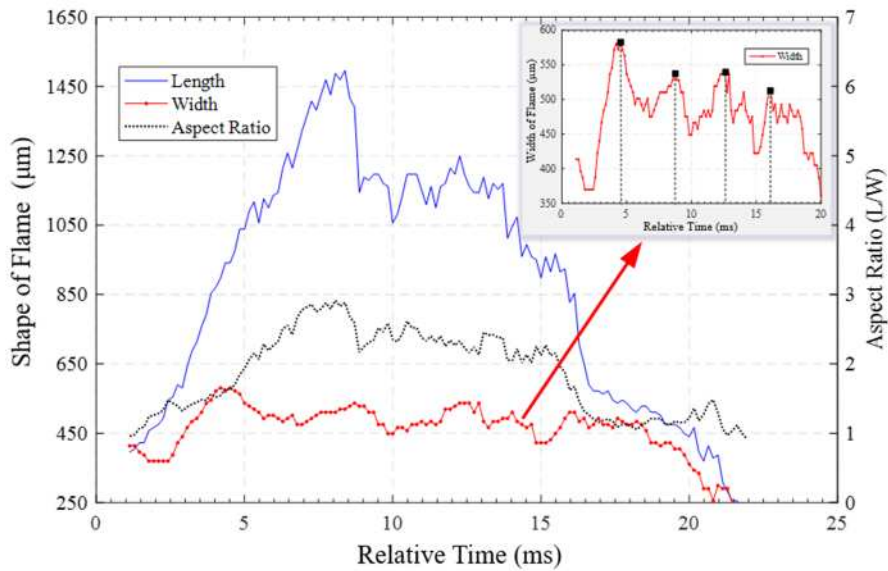
1 μm . In the volatile combustion phase (about 1–20 ms), A_o and A_c , increase rapidly at the beginning
 2 and reach the maximum at 8 ms and then decrease to the minimum quickly. In this phase, the area
 3 of the combustion zone could increase to approximately 10 times bigger than that of the char
 4 particle [11, 16, 21]. A_p increases gradually after experiencing a short-lived decreasing period
 5 (22–26 ms, after the devolatilisation phase). This short-lived decreasing period is due to the fact
 6 that the volatile matter was burned out before the remaining char had not reached its ignition
 7 point, and thus, the brightness of the particle remains low. The area of the coal particle reduces
 8 gently in the char combustion phase as the combustion of carbon requires more time than
 9 volatiles. As it can be deduced from the peak points in figure 7, A_p varies periodically at
 10 approximately 260 Hz and 210 Hz during 7–20 ms and 25–40 ms in, respectively. This may be
 11 attributed to the particle rotation in the direction perpendicular to the imaging plane, which was
 12 also demonstrated by Bai *et al.* [17]. The results in figure 7 demonstrate that the particle rotated
 13 more quickly in the volatile combustion phase than in the char combustion phase due to the release
 14 and combustion of volatiles. Such a phenomenon may be due to the release and combustion of
 15 volatiles. However, more evidence about the rotation of a coal particle during combustion should
 16 be obtained to support the above analysis by more sophisticated imaging techniques, such as 3-D
 17 imaging.



18
 19 **Figure 7.** Areas of the combustion zone of coal particle

20 The variation of length, width and aspect ratio of the volatile flame is illustrated in figure 8. As
 21 it can be seen, the length of the volatile flame increased gradually to a stable value in 5–14 ms
 22 with the continuous release and combustion of the volatile matter. The flame skews downward
 23 because that, in the test, the secondary air flow was introduced from the top of the furnace (at a
 24 flow rate of 5 l min^{-1} , to ensure the complete combustion [17]). It is noticeable that a significant

1 increase in the flame length occurred from 6.5 ms to 9 ms due to the combustion of a wisp of
 2 volatiles (at 7.1 ms, figure 5(b)). This phenomenon may be caused by the sudden release of
 3 volatile matter, change of volatile composition, the mixing between air and volatile, etc.
 4 Furthermore, during the volatile combustion, the width of flame varies in the range of 420–580
 5 μm periodically with a mild decreasing trend, as shown in figure 8. The particle width reaches the
 6 peak value at 4.5 ms, 8.6 ms, 12.5 ms and 16.1 ms, respectively. Therefore, the width of volatile
 7 flame fluctuated at a frequency of about 250 Hz and the flame swinging frequency is about 125
 8 Hz. This phenomenon suggests that the swing of the volatile flame tail may be influenced by the
 9 rotation of the solid particle (figure 7) or the interactions between the particle and surrounding air
 10 flow. The variation trend of the aspect ratio of the volatile flame is consistent with that of the
 11 flame length, although the width of the volatile flame has noticeable periodic changes.

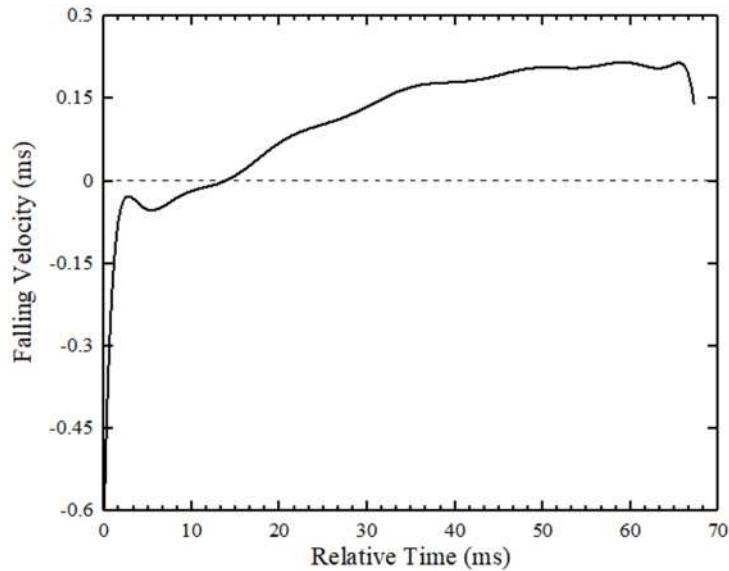


12
 13 **Figure 8.** Length, width and aspect ratio of the volatile flame.

14 3.3.3 Falling velocity

15 Figure 9 represents the velocity of the coal particle (calculated from the time that the particle
 16 can be identified in images). It can be seen from figure 9 that the coal particle did not fall
 17 continually during the combustion process, but with an unexpected short-term slow upward
 18 movement in until 14 ms. During this short period, the velocity of the particle decreased rapidly
 19 from about 0.5 m s^{-1} and then slowly decreased to 0 (ending the upward motion). In the volatile
 20 combustion phase, the coal particle was primarily subjected to three forces in the vertical
 21 direction, i.e. the downward gravity and drag force of hot laminar air flow, and the upward
 22 buoyancy generated by the combustion of volatiles below the coal particle (as the bottom part of
 23 the particle enters the furnace). Therefore, the upward motion occurred when the upward
 24 buoyancy is stronger than the two opposite forces. Due to the upward movement, it took about 25
 25 ms for the coal particle to return to its initial position, which almost covered the entire volatile

1 combustion process. The coal particle began to fall and the velocity increased slowly from 14 ms
2 until 48 ms. Hereafter, the particle velocity remained at a constant value of about 0.19 m s^{-1} , which
3 was consistent with the variation of particle brightness in the steady char combustion phase (figure
4 6).



5
6 **Figure 9.** Falling velocity of the coal particle.

7 **5. Conclusions**

8 The proposed methodology has performed well for the quantitative characterisation of the
9 combustion behaviours of individual coal particles. The improved-Canny extraction algorithm is
10 capable of extracting the whole combustion zone of a coal particle. The combination of the
11 improved-Canny and Otsu algorithms for extracting the solid fuel particle in the volatile
12 combustion phase has also been achieved. A set of physical parameters that are determined from
13 the processed images has shown its effectiveness in quantifying the combustion process of a coal
14 particle. Experimental results have demonstrated that the combustion of the volatiles and char
15 occurs successively for the investigated bituminous coal while the volatile matter burns rapidly
16 in a large area with a lower ignition point. Under the influence of the release and combustion of
17 volatile, the coal particle rises for about 14 ms in the early phase of the combustion before falling
18 continuously. The coal particle rotates during combustion with a rotation frequency being slightly
19 higher in the volatile combustion phase than that in the char combustion phase according to the
20 variation of the area of the combustion zone. Additionally, the volatile flame tail swings at about
21 125 Hz depending on the rotation of the unburned part of the coal particle.

22 **Acknowledgments**

23 This work is supported by the National Natural Science Foundation of China (No. 51827808),
24 Fundamental Research Funds for the Central Universities (2019MS023) from North China
25 Electric Power University and the International Clean Energy Talent Program (iCET) of the China

1 Scholarship Council. Drs Tom Bennet and Archi Sarroza are acknowledged for their contribution
2 to the data collection of this study by conducting the V-DTF test described in this paper.

3 **References**

- 4 [1] BP p.l.c. 2018 BP Statistical Review of World Energy
- 5 [2] Žajdlík R, Jelemenský L, Remiarová B and Markoš J 2001 Experimental and modelling
6 investigations of single coal particle combustion *Chem. Eng. Sci.* 56 1355–1361
- 7 [3] Levendis Y A, Joshi K, Khatami R and Sarofim A F 2011 Combustion behavior in air of single
8 particles from three different coal ranks and from sugarcane bagasse *Combust. Flame* 158 452–
9 465
- 10 [4] Jiang X, Chen D, Ma Z and Yan J 2017 Models for the combustion of single solid fuel particles
11 in fluidized beds: A review *Renew. Sust. Energ. Rev.* 68 410–431
- 12 [5] Zhang M, Yu J and Xu X 2005 A new flame sheet model to reflect the influence of the oxidation
13 of CO on the combustion of a carbon particle *Combust. Flame* 143 150–158
- 14 [6] Sadhukhan A K, Gupta P and Saha R K 2010 Modelling of combustion characteristics of high
15 ash coal char particles at high pressure: Shrinking reactive core model *Fuel* 89 162–169
- 16 [7] Köser J, Becker L G, Goßmann A-K, Böhm B and Dreizler A 2017 Investigation of ignition and
17 volatile combustion of single coal particles within oxygen-enriched atmospheres using high-
18 speed OH-PLIF *Proc. Combust. Inst.* 36 2103–2111
- 19 [8] Farazi S, Sadr M, Kang S, Schiemann M, Vorobiev N, Scherer V and Pitsch H 2017 Resolved
20 simulations of single char particle combustion in a laminar flow field *Fuel* 201 15–28
- 21 [9] Jiang X, Yang H and Liu H 2002 Analysis of the effect of coal powder granularity on combustion
22 characteristics by thermogravimetry *Proceeding of the CSEE* 22 142–145
- 23 [10] Shan L, Kong M, Bennet T D, Sarroza A C, Eastwick C, Sun D, Lu G, Yan Y and Liu H 2018
24 Studies on combustion behaviours of single biomass particles using a visualization method
25 *Biomass and Bioenergy* 109 54–60
- 26 [11] Shaddix C R and Molina A 2009 Particle imaging of ignition and devolatilization of pulverized
27 coal during oxy-fuel combustion *Proc. Combust. Inst.* 32 2091–298
- 28 [12] Wagner D R, Holmgren P, Skoglund N and Brostrom M 2018 Design and validation of an
29 advanced entrained flow reactor system for studies of rapid solid biomass fuel particle conversion
30 and ash formation reactions *Rev. Sci. Instrum.* 89 065101
- 31 [13] Schiemann M, Geier M, Shaddix C R, Vorobiev N and Scherer V 2014 Determination of char
32 combustion kinetics parameters: Comparison of point detector and imaging-based particle-sizing
33 pyrometry *Rev. Sci. Instrum.* 85 075114
- 34 [14] Riaza J, Khatami R, Levendis Y A, Álvarez L, Gil M V, Pevida C, Rubiera F and Pis J J 2014
35 Single particle ignition and combustion of anthracite, semi-anthracite and bituminous coals in air
36 and simulated oxy-fuel conditions *Combust. Flame* 161 1096–1108
- 37 [15] Lee H and Choi S 2016 Motion of single pulverized coal particles in a hot gas flow field *Combust.*
38 *Flame* 169 63–71
- 39 [16] Lee H and Choi S 2018 Volatile flame visualization of single pulverized fuel particles *Powder*

- 1 *Technol.* 333 353–363
- 2 [17] Bai X, Lu G, Bennet T D, Sarroza A C, Eastwick C, Liu H and Yan Y 2017 Combustion behavior
3 profiling of single pulverized coal particles in a drop tube furnace through high-speed imaging
4 and image analysis *Exp. Therm. Fluid Sci.* 85 322–330
- 5 [18] Sarroza A C, Bennet T D, Eastwick C and Liu H 2017 Characterising pulverized fuel ignition in
6 a visual drop tube furnace by use of a high-speed imaging technique *Fuel Process. Technol.* 157
7 1–11
- 8 [19] Chaves D, Fernández-Robles L, Bernal J, Alegre E and Trujillo M 2018 Automatic
9 characterization of char from the combustion of pulverized coals using machine vision *Powder
10 Technol.* 338 110–118
- 11 [20] Wu Y, Yao L, Wu X, Chen J, Gréhan G and Cen K 2017 3D imaging of individual burning char
12 and volatile plume in a pulverized coal flame with digital inline holography *Fuel* 206 429–436
- 13 [21] Yao L, Wu C, Wu Y, Chen L, Chen J, Wu X and Cen K 2019 Investigating particle and volatile
14 evolution during pulverized coal combustion using high-speed digital in-line holography *Proc.
15 Combust. Inst.* 37 2911–2918
- 16 [22] Zhang Y, Liu X and Li F H 2007 Self-adaptive image histogram equalization algorithm *J.
17 Zhejiang Univ. (Eng. Sci.)* 41 630–633 (in Chinese)
- 18 [23] N. Otsu 1979 A threshold selection method from gray-level histograms *IEEE T Syst. Man
19 Cybern.* 9(1) 62–66
- 20 [24] Gonzalez R C and Woods R E 2007 Digital Image Processing (3rd Edition) *Prentice Hall, Inc.,
21 Upper Saddle River, U. S.*
- 22 [25] Gonzalez R C, Woods R E and Eddins SL 2009 Digital Image processing Using MATLAB (2nd
23 Edition) *Gatesmark Publishing, L. L. C., Knoxville, U. S.*
- 24 [26] Canny J 1986 A Computational approach to edge detection *IEEE T. Pattern Analy.* 8 679–698
- 25 [27] Wang G, Tse P W and Yuan M 2018 Automatic internal crack detection from a sequence of
26 infrared images with a triple-threshold Canny edge detector *Meas. Sci. Technol.* 29 025403